Am J Nucl Med Mol Imaging 2023;13(4):147-155
www.ajnmmi.us /ISSN:2160-8407/ajnmmi0151544

Original Article

Evaluation of enhanced permeability effect and different linear energy transfer of radionuclides in a prostate cancer xenograft model

Oskar Vilhelmsson Timmermand[1], Marcella Safi[1], Bo Holmqvist[2], Joanna Strand[1,3]

[1]Department of Oncology, Lund University, Lund, Sweden; [2]ImaGene-iT AB, Medicon Village, Lund, Sweden; [3]Department of Hematology, Oncology, Radiation Physics, Skåne University Hospital, Lund University, Lund, Sweden

Received June 1, 2023; Accepted July 30, 2023; Epub August 15, 2023; Published August 30, 2023

Abstract: We have previously investigated the biodistribution and therapy effect of a humanized monoclonal antibody targeting free prostate-specific antigen (fPSA) intended for theranostics of hormone-refractory prostate cancer. In the present study, we evaluated the off-target effect and different linear energy transfer (LET) radionuclides without the effect of PSA targeting by using an antibody with the same scaffold as previously used immunoconjugates but with random, non-specific, antigen binding region. This allows us to identify alterations generated by specific targeting and those related to passive bystander effects, such as enhanced permeability and retention (EPR). A control humanized IgG monoclonal antibody (hIgG1) and an isotype control IgG monoclonal antibody were conjugated with the chelator CHX-A"-DTPA. The immunoconjugate was radiolabeled with either Lutetium-177 ([^{177}Lu]Lu) or Indium-111 ([^{111}In]In). A biodistribution study in mice carrying LNCaP xenografts, was performed to evaluate the non-specific uptake of [^{177}Lu]Lu-hIgG1 in tumors and normal organs. Further, therapy studies of [^{177}Lu]Lu and [^{111}In]In labeled IgG were performed in BALB/c mice carrying LNCaP xenografts. Tumor tissues of treated xenografts and control were sectioned and immunohistochemically stained for Ki67 and PSA. The highest tumor uptake for the [^{177}Lu]Lu-hIgG1 was seen at 72 hours (7.2±2 %IA/g), when comparing the tumor uptake of the fPSA targeting antibody to the non-specific antibody, the non-specific antibody contributes to half of the tumor uptake at 72 h. The liver uptake was 3.1±0.5 %IA/g at 24 h, 2.8±0.5 %IA/g at 72 h and 1.3±0.6 %IA/g at 120 h in LNCaP xenografts, which was approximately three times lower at 24 h and two times lower at 72 h than for the antibody with preserved targeting. Immunohistochemical labeling showed a reduction of PSA expression and a reduction of Ki67 labeled cells in the [^{111}In]In treated LNCaP tumors, compared to vehicle and [^{177}Lu]Lu treated mice. In conclusion, we found that specific targeting might negatively influence normal organ uptake when targeting secreted antigens. Furthermore, different energy deposition i.e. linear energy transfer of a radionuclide might have diverse effects on receptor expression and cell proliferation in tumors.

Keywords: PSA, prostate cancer, radionuclide therapy, enhanced permeability and retention effect, linear energy transfer

Introduction

Most conventional cancer therapies (e.g., chemotherapy, external radiotherapy) rely on relatively more damage to populations of cells that show uncontrolled growth. However, these treatments are nonselective [1]. There has been an emphasis on developing "targeted therapies" designed to limit off-target damage by homing in on more cancer-specific traits, such as the high expression of proteins or pathways more or less absent in healthy tissues [2].

One class of targeting oncology therapeutics is monoclonal antibodies (mAbs). Monoclonal antibodies display high specificity for their target, the ability to engage and activate the immune system, easy production, and an-in general-already well-established safety profile [3, 4]. Thus, mAbs are well suited for targeted cancer therapy and can be conjugated with cytotoxic payloads, such as toxins or radionuclides, to enhance their anti-tumor capabilities [5]. However, several characteristics influence the success of antibody-drug conjugates

(ADCs). ADCs can suffer or benefit from their non-specific accumulation in tissue, that is, influencing off-target effects on tumor uptake. One mechanism behind non-specific tumor uptake is the enhanced permeability and retention effect (EPR), typical for all agents with a size greater than 45 kDa [6]. The EPR effect is characterized by an increased accumulation of macromolecules, such as antibodies, in tumors due to leaky tumor vasculature and dysfunctional lymphatic system [7]. The EPR effect can limit the use of monoclonal antibodies as imaging agents due to high non-specific accumulation in nontarget expressing tumors or organs such as the liver and spleen. Unspecific tumor accumulation has been shown in several preclinical studies with radiolabeled antibodies [8, 9]. Given the high tumor retention seen for non-specific antibodies, we here investigated whether the EPR in tumors could contribute to any substantial therapy effect in prostate cancer xenografts in mice and if there were any differences in therapy effect between high and low high linear energy transfer (LET) radionuclides. The extremely short range for Auger electrons and high linear energy transfer makes Auger electrons attractive for radiation treatment of cancer, especially if they are emitted near the DNA of cancer cells. Since Auger electrons do not suffer from any crossfire effect, radiotoxicity in normal organs is limited. However, the crossfire effect from the longer range β-emitters, such as [^{177}Lu]Lu (t1/2=6.7 d; Emax=0.5 MeV), can kill non-targeted cells within the range of the β-particles increasing homogenous absorbed distribution within the whole tumor, targeting all cells [10].

We have previously shown specific in vivo binding and therapy effects in LNCaP xenografts of a humanized monoclonal antibody targeting free prostate-specific antigen (fPSA) labeled with either [^{111}In]In, [^{225}Ac]Ac or [^{177}Lu]Lu [11-13]. In the present study, we studied the effects on antibody tumor and organ retention separated from specific targeting. We did this by radiolabeling an antibody with the same scaffold and retained Fc-part as the specific antibody previously used but with a random, non-specific, antigen-binding region and performed a biodistribution study in mice carrying a prostate-specific antigen expressing cell line. Furthermore, a random human IgG was radiolabeled with a beta or an Auger emitter, and the therapeutic efficacy was investigated with regard to changes in PSA expression, the most important marker of prostate cancer.

Materials and methods

Conjugation

hIgG1 (Innovagen AB) and IgG (Native Human IgG, Abcam, Cambridge, United Kingdom) were conjugated with p-SCN-CHX-A"-DTPA (DTPA) at a 12:1 chelator-to-antibody molar ratio. Buffer exchange was conducted on PBS solutions of the antibodies. This was done by first equilibrating NAP-5 columns (GE Healthcare, Uppsala, Sweden) with 0.07 M sodium borate buffer pH 9.2 (Sigma Aldrich) and then eluting the antibodies on the columns using the same buffer. The reaction vial was incubated at 38°C overnight. The immunoconjugates were separated from free chelate by size-exclusion chromatography using a NAP-5 column, pre-equilibrated with 20 mL, 0.2 M, pH 5.5 ammonium acetate buffer (Sigma Aldrich), through elution with 1 mL of the same ammonium acetate buffer. Aliquots were stored at -20°C before labeling.

Radiolabeling

For *in vivo* experiments, hIgG1 and IgG conjugated to CHX-A"-DTPA in a 12:1 chelator-to-antibody molar ratio were labeled with [^{111}In]In or [^{177}Lu]Lu. Approximately 30-50 μg of IgG were mixed with a solution of approximately 15-20 MBq [^{111}In]$InCl_3$ (Mallinkrodt, Railroad Avenue, Hobart, NY, USA) in the presence of 0.2 M ammonium acetate buffer, pH 5.5. The mixture was vortexed and incubated at 38°C for 1 h. For labeling with [^{177}Lu]Lu (Curium, Stockholm, Sweden), 30-50 μg of IgG or hIgG1 was mixed with [^{177}Lu]$LuCl_3$ (15-25 MBq) in ammonium acetate buffer and incubated at 38°C for 1 h as above. The radiolabeled antibodies were purified using AMICON Ultra-0.5-centrifugal filter devices with a MWCO 30,000 Da (Millipore, Burlington, MA, USA). The labeling yield and purity of the radiolabeled antibodies were determined using ITLC strips (150-771 DARK GREEN Tec-Control Chromatography strips), Biodex Medical Systems (Ramsey Road Shirley, NY, USA), eluted with 0.2 M citric acid and measured using the Cyclone Storage Phosphor System (PerkinElmer, Waltham, MA, USA). The radiolabeled antibodies were

remained at the origin, while free [^{111}In]In or [^{177}Lu]Lu moves to the front. All radiolabeled antibodies were purified from non-bound [^{111}In]$InCl_3$ or [^{177}Lu]$LuCl_3$ using a size-exclusion NAP-5 column (Thermo Fischer Scientific, Waltham, MA, USA) equilibrated with PBS (Hyclone).

Ethical concern

All animal experiments were performed in accordance with national legislation on laboratory animal protection and permitted by the local Ethics Committee for Animal Research at Lund University (permit number 4350-20). All animals were housed under controlled conditions with free access to water and standard rodent chow. The cages were equipped with cardboard tunnels and shavings. Euthanasia was performed under Ropmpun/Ketalar anesthesia, and all efforts were made to minimize suffering. If the tumor diameter reached > 15 mm or a volume of over 1000 mm^3 or a weight loss of 20% or if a severe decline in general condition (e.g. ruffled fur, paralysis) was noticed, animals were immediately euthanized.

Prostate cancer tumor model

Balb/c nude mice (Janvier) were used for the therapy studies. LNCaP cells (5-7 × 10^6 cells per mouse) (Prostate Carcinoma cells Clone FGC ATCC®CRL-1740, Lot 5972254) were implanted subcutaneously (s.c.), in a 200 µL cell suspension (1:1 mixture of Matrigel, Corning, and RPMI 1640 medium), on the right hind leg 3-4 weeks before the experiment. After implantation, the animals were monitored daily for signs of illness. Thereafter, the animals were monitored once a week for tumor growth, body weight, and physical signs of illness during the full time of the study.

Biodistribution of [^{177}Lu]Lu-hIgG1 in Balb/c nude mice bearing LNCaP prostate cancer xenografts

The unspecific antibody hIgG1 labeled with [^{177}Lu]Lu was injected into 3 groups of mice (n=4) (32 µg/mice, 140 kBq/mice) carrying s.c. LNCaP xenografts. The mice were sacrificed at 24, 72, and 120 h p.i. using an overdose of anesthesia: Ketalar (50 mg/mL; Pfizer), Rompun (20 mg/mL; Bayer), followed by heart puncture and exsanguination with a syringe.

Blood, lung, liver, spleen, stomach, small intestine, large intestine, kidney, tumor, muscle, bone, brain, and carcass were collected and weighed, and their radioactivity concentration in the respective tissue was measured in a NaI(Tl) automated well counter (PerkinElmer, USA). The data were corrected for background radiation and decay during measurement. Organ uptake values were calculated as percent of injected activity per gram of tissue (%IA/g).

Therapeutic efficacy

A therapy study was conducted to evaluate the difference in therapeutic efficacy between an Auger-emitting radionuclide and a beta-emitting radionuclide labeled to an antibody without targeting specificity. Three groups of mice carrying LNCaP tumors were administered a single iv injection of either PBS (n=6), 20-21 MBq [^{177}Lu]Lu labeled IgG (n=7) or 24 MBq [^{111}In]In labeled IgG (n=9). Body weight and tumor volume (external caliper measurement, V=0.5 × length × width × width) were monitored once per week during the whole experiment (7 weeks).

Immunohistochemistry

Tumor sections from the therapy experiments were immunohistochemically labeled for Ki67 and PSA. The tumors were dissected out between 14-32 days post-injection. The presence of labeling (Ki67 labeled cell nuclei and PSA labeled cytoplasm) of viable tumor cells and tissue necrosis was assessed in a bright-field microscope and semi-quantified (blinded by two histologists).

Tumor tissue was collected from mice and was fixed by immersion in 4% paraformaldehyde overnight at room temperature (RT). Tissues were then dehydrated in an alcohol serial (70-99%) and ended in 100% Xylen. Tissues were then infiltrated in paraffin solution and embedded in paraffin. Parallel sections (4 µm) were made that were collected on SuperFrost Plus microscope slides (six sections per staining and immunolabeled).

For the immunohistochemical labeling, sections were rehydrated, starting with 100% Xylen followed by a grade alcohol serial, and ending in distilled H_2O. Epitope retrieval was

Table 1. Radiolabeling yield for the different radio immunoconjugates (Mean ± SD)

Conjugate	Yield	After purification
[^{177}Lu]Lu-IgG	94±0.6%	-
[^{111}In]In-IgG	99±2.1%	-
[^{177}Lu]Lu-hIgG1	57±2.9%	99%

performed in TRIS buffer (1 mM, pH 9.0) for 4 min reaching about 99°C. After rinses in H_2O and PBS, tissues were quenched with 0.3% H_2O_2 (in PBS) for 10 min at RT. Following rinses in PBS (3 × 3 min), blocking was performed with 1% BSA and 0.05% Triton X-100 (PBSBSATX) for 30 min at RT.

Parallel sections were then incubated with rabbit monoclonal primary antibodies made against PSA (ab240982, Abcam, diluted 1:200) or against Ki67 (MA5-14520, Thermo Fischer Scientific, diluted 1:150) for 90 min at RT. Primary antibody specificity was tested by omitting the primary antibody incubation from the protocol in parallel sections to those incubated with primary antibodies.

Sections were rinsed in PBS (3 × 3 min) and incubated with HRP-conjugated secondary antibodies made in goat (Vector Laboratories USA, MP-7451) for 30 min at RT. All antibody incubations were performed in a moisture chamber. Following rinses in PBS (3 × 3 min), the immunoreaction was performed in a solution containing 3,3'-Diaminobenzidine (DAB, 0.5% in PBS) and H_2O_2 (0.1%) for 10 min at RT. After rinsing in PBS (3 × 3 min) and distilled water, sections were counterstained with Mayers hematoxylin and then rinsed in distilled water. Sections were dehydrated in a graded alcohol serial (70-99.9%, 2 × 2) ended with Xylen (100%, 2 × 5 min) and were then mounted and cover-slipped in Pertex (Histolab, Gtbg, Sweden).

The histopathological assessment of tissue and evaluation of the immunohistochemical label was performed in a bright-field microscope (Olympus IX73). Six parallel sections from three animals per treatment group were analyzed. The number of labeled cells in the sections was scored (independently by two different observers), and the number of cells per section was graded on a scale from no (0) to high (3) number. Furthermore, histopathological assessment with regard to surrounding bleeding (B/O) expressed as a percentage of the total area around the tumor, as well as intratumoral bleeding (B/T), and necrosis and immune cell infiltration was graded as none (0) to high (3). Representative images were grabbed with a DP80 Olympus detector.

Statistical analysis

An unpaired *t*-test was used for comparison of the biodistribution of different conjugates. A *p*-value of < 0.05 was considered statistically significant.

Results

Radiolabeling

The labeling with [^{177}Lu]Lu and [^{111}In]In to IgG provided a high yield, over 94%. The labeling efficiency of [^{177}Lu]Lu to hIgG1-conjugate was somewhat lower, 57±2.9% (**Table 1**). After purification, the radiochemical purity was over 98% for [^{177}Lu]Lu-hIgG1.

Biodistribution of [^{177}Lu]Lu-hIgG1 in Balb/c nude mice bearing LNCaP prostate cancer xenografts

The results of the biodistribution are presented in **Figure 1**. The tumor uptake for [^{177}Lu]Lu-hIgG1 in LNCaP xenografts was 6.1±0.78 %IA/g at 24 h and 7.2±2 %IA/g 72 hours and 3.88±0.99 %IA/g at 120 h. For the antibody with preserved targeting the tumor uptake in the same experimental setting was 11.3±0.4 %IA/g at 24 h and 15.1±2.3 %IA/g at 72 h. The antibody with preserved antigen targeting hade significant higher ($P < 0.05$) tumor uptake compared to the unspecific antibody at 24 h and 72 h, however the unspecific uptake contributed to almost half of the tumor uptake at these time points.

The [^{177}Lu]Lu-hIgG1 demonstrated rapid clearance from blood 3.9±2.4 %IA/g at 120 h and low uptake in normal organs and tissues.

The liver uptake was considerably low for all time points and showed fast clearance (3.1±0.5 %IA/g at 24 h, 2.8±0.5 %IA/g at 72 h and 1.3±0.6 %IA/g at 120 h). When compared to published data of the same antibody scaffold with preserved antigen targeting to fPSA, the liver uptake was significantly lower (P <

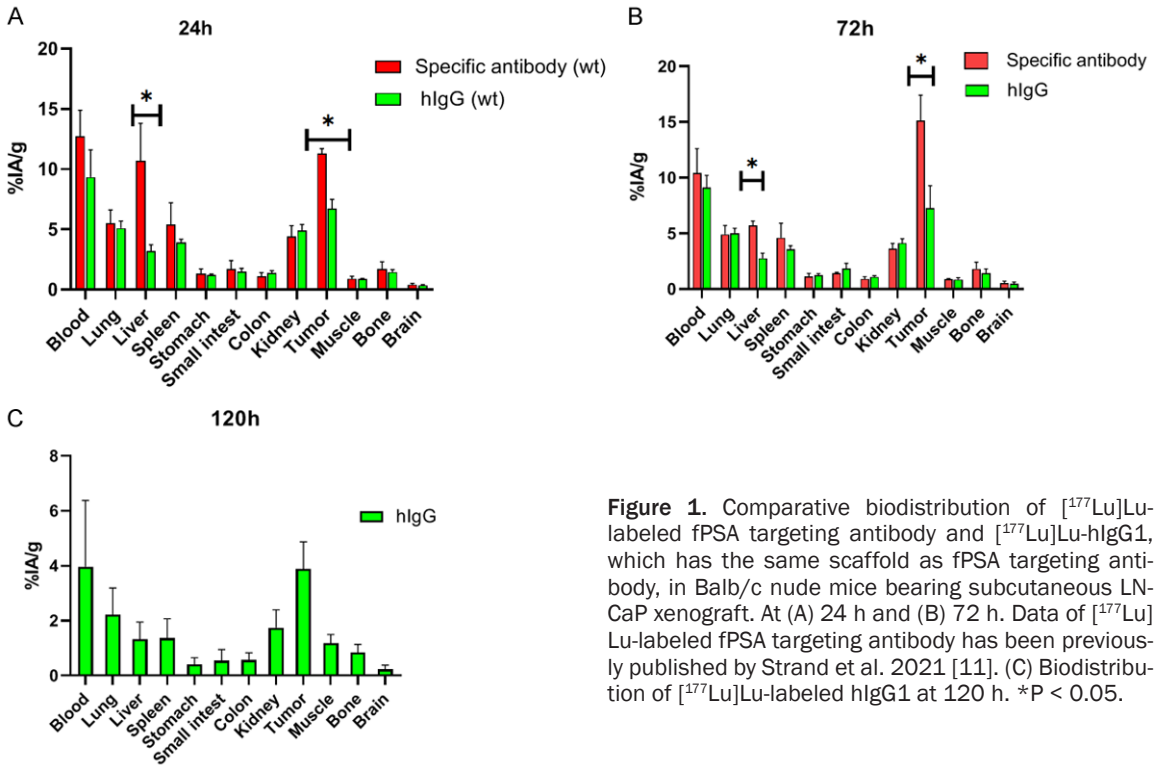

Figure 1. Comparative biodistribution of [^{177}Lu]Lu-labeled fPSA targeting antibody and [^{177}Lu]Lu-hIgG1, which has the same scaffold as fPSA targeting antibody, in Balb/c nude mice bearing subcutaneous LNCaP xenograft. At (A) 24 h and (B) 72 h. Data of [^{177}Lu]Lu-labeled fPSA targeting antibody has been previously published by Strand et al. 2021 [11]. (C) Biodistribution of [^{177}Lu]Lu-labeled hIgG1 at 120 h. *P < 0.05.

0.05), approximately 3 times lower at 24 h, 3.1±0.5 %IA/g vs. 10.7±3.1 %IA/g, for the non-specific antibody (**Figure 1**) and 2 times lower (2.7±0.5 %IA/g vs. 5.7±0.4 %IA/g) at 72 h [11]. There was no other significant difference in organ uptake between the unspecific antibody and the antibody with preserved antigen binding.

Therapy

Figure 2A-C display tumor growth for each mouse. Some subjects (n=5) had to be euthanized preterm due to non-tumor size-related health issues (poor health). The tumor growth between the groups is displayed in **Figure 2D**. There were no significant difference in tumor growth between the different groups.

Immunohistochemistry

Histological scoring of Ki-67 and PSA immunoreactive viable cells in tumor tissue treated with [^{177}Lu]Lu-IgG or [^{111}In]In-IgG is shown in **Table 2**. The control group (PBS) had a relatively high number of Ki67 and PSA immunoreactive cells, whereas tumor bleeding and surrounding bleeding were relatively low. The tumors treated with [^{111}In]In-IgG had a low number of Ki67 and PSA immunoreactive cells. The [^{177}Lu]Lu-IgG treated group had relatively higher numbers of both Ki67 and PSA immunoreactive cells, as compared to the [^{111}In]In-IgG group. Representative images illustrating the immunohistochemical labeled result of PSA and Ki67 in [^{177}Lu]Lu-IgG and [^{111}In]In-IgG are shown in **Figure 3**.

Discussion

We have previously shown that a specific humanized antibody targeting fPSA possesses specific and high binding to LNCaP xenografts [11]. The [^{177}Lu]Lu labeled fPSA targeting antibody has high uptake and slow clearance from the liver in mice carrying LNCaP xenografts; the same was also seen when labeled with [^{225}Ac]Ac [13]. In the present study, we therefore investigated the potential contribution of unspecific uptake. We repeated our previous experimental setting for the specific antibody targeting fPSA, but instead, we used a control monoclonal antibody with the same scaffold as for the specific antibody.

The accumulation of antibodies in the liver is related to the catabolism and FcRn-mediated recirculation of antibodies [14]. Interestingly, in

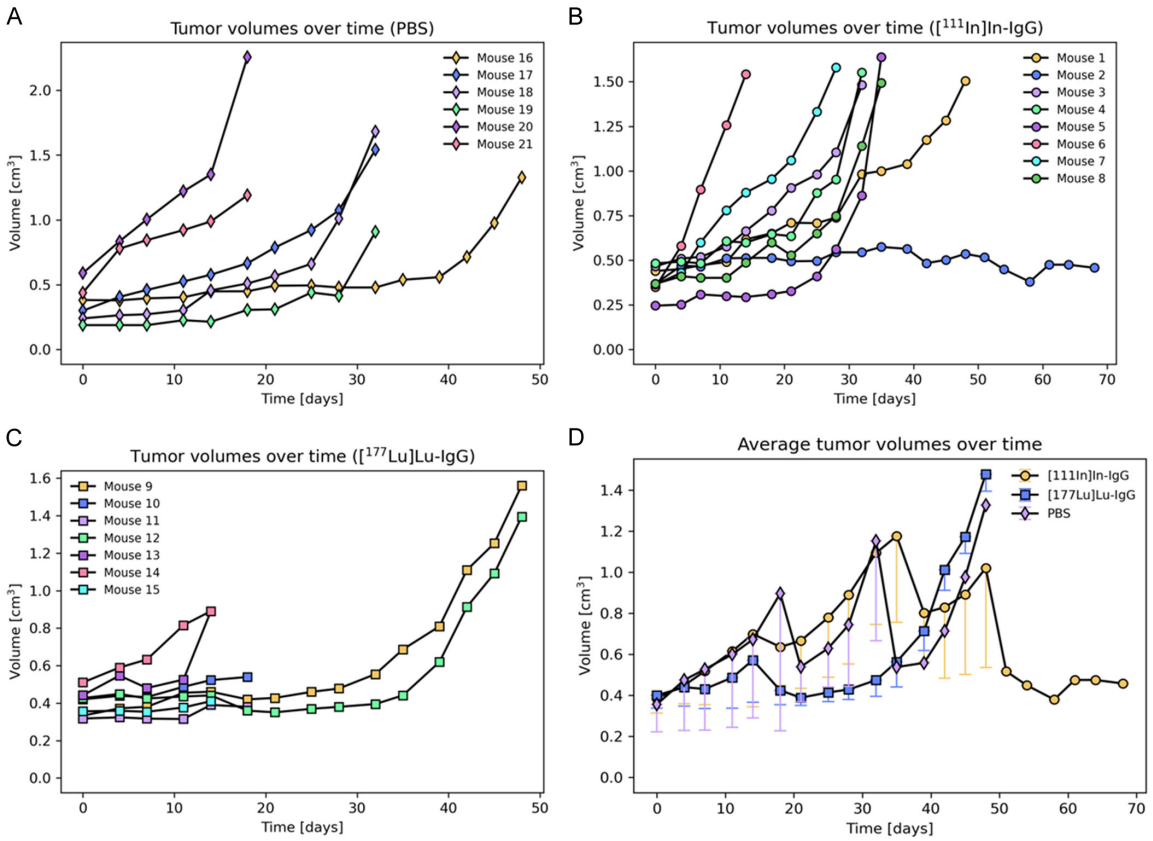

Figure 2. A-C: The image showes the individual tumor growth in each group. A: PBS. B: [^{111}In]In-IgG. C: [^{177}Lu]Lu-IgG displayed as volume (cm^3). D: The therapy efficacy for [^{177}Lu]Lu-IgG conjugates, Vehicle (PBS), and [^{111}In]In-IgG conjugates.

Table 2. The table shows the scoring results from histopathological assessment and analyses of immunohistochemical labeling of treated tumors with either PBS (control), [^{111}In]In-IgG, or [^{177}Lu]Lu-IgG conjugated at chelate to antibody molar ratio of 12:1

Group (n=3)	Days (d) after injection	B/O (%)	B/T (0-3)	Necrosis (0-3)	Infiltr (0-3)	PSA (0-3)	Ki67 (0-3)
PBS	1=32 d 2=48 d 3=18 d	0-20	1	1	1	3	3
[^{111}In]In-IgG	1=32 d 2=14 d 3=28 d	50	3	2	1	0	1
[^{177}Lu]Lu-IgG	1=14 d 2=18 d 3=48 d	30-50	3	2	2	3	3

Histopathological assessment has been made based on four aspects: surrounding bleeding (B/O) expressed as a percentage (%) of the total area around the tumor, internal tumor bleeding (B/T), necrosis and immune cell infiltration (Infiltr), Ki67, and PSA immunohistochemical labeling of viable cells was graded 0-3 (non to high).

the present study, the liver uptake for the unspecific antibody with the same scaffold and preserved FcRn binding as the fPSA targeting antibody was approximately 3 times lower (3.1±0.5 %IA/g vs. 10.7±3.1 %IA/g) at 24 h and 2 times lower (2.7±0.5 %IA/g vs. 5.7±0.4 %IA/g) at 72 h (**Figure 1**). Formation of soluble immunocomplexes between radioimmunoconjugates and secreted antigen as fPSA have shown to increase liver uptake, which might explain the higher liver uptake for the fPSA targeting antibody [15]. Further, catabolism of PSA is believed

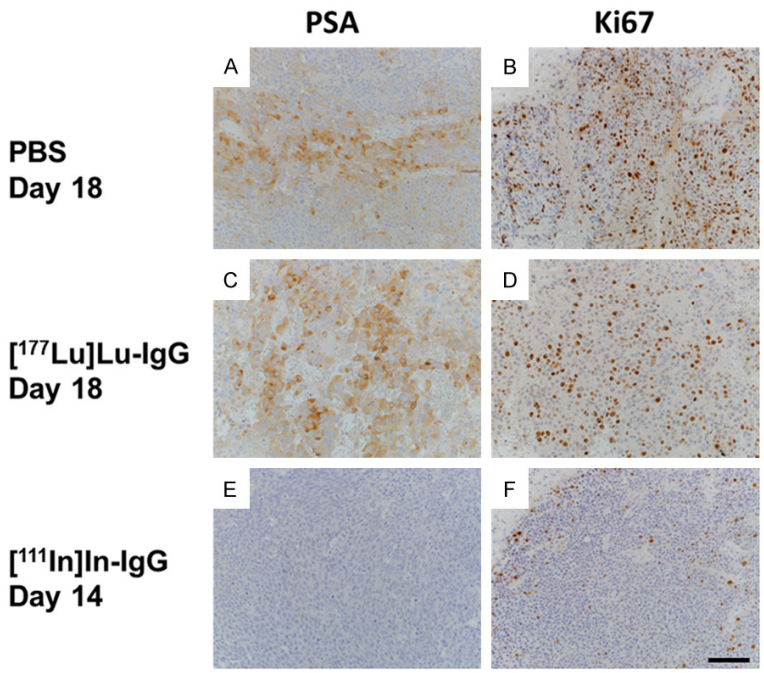

Figure 3. Representative images illustrating the immunohistochemical labeled result of PSA and Ki67 in [^{177}Lu]Lu-IgG and [^{111}In]In-IgG treated and untreated (PBS) tumors (see also **Table 1**). Scale bar shown in (F), for (A-F). Scale bar represent 100 µm. Images demonstrate the high content of PSA positive cells in PBS treated (A) and [^{177}Lu]Lu-IgG treated tumors (C), compared to the lack of PSA positive cells present in [^{111}In]In-IgG treated animals (E). Images also demonstrate the high number of Ki67 positive cells in PBS treated (B) and relatively lower presence of Ki67 positive cells in [^{177}Lu]Lu-IgG treated (D), as well as the few Ki67 positive cells in the [^{111}In]In-IgG treated (F) tumors.

to mainly take place in the liver [16] and model system deprived of fPSA are therefore important when evaluating the therapeutic efficacy of such radioimmunoconjugates. As PCa liver metastases are associated with shorter overall survival time [17], low unspecific uptake in the liver is important for the detection of liver metastases. Furthermore, slow clearance from the liver could also contribute to hepatic radio toxicity when using alfa or beta-emitting therapeutic radionuclides.

The tumor uptake for the unspecific antibody was at its highest at 72 h (7.1±2 %IA/g) in LNCaP xenografts. When comparing the tumor uptake of the fPSA targeting antibody to the non-specific antibody, the non-specific antibody contributes to half of the tumor uptake at 24 h and 72 h; contributing to the unspecific uptake could be both blood activity concentration and potential accumulation via the EPR effect.

As the tumor retention was relatively high for the non-specific antibody, we investigated whether the EPR effect in tumors could contribute to any substantial therapy effect in prostate cancer xenografts in mice and whether there was any difference in therapeutic effect and histological changes between high and low LET. We, therefore, performed two therapy studies with either [^{111}In]In labeled unspecific IgG or [^{177}Lu]Lu labeled unspecific IgG in mice carrying LNCaP xenografts.

Surprisingly, the immunohistochemical data showed that treatment with [^{111}In]In labeled IgG (24 MBq per mouse) in LNCaP xenografts caused a clear reduction in cell proliferation and possible increased cell death of PSA expressing cells due to the absorbed dose delivered. This might be a result of internalization of the complex. However, the histopathological assessment did not show any significant tumor retardation in the group. The animals tolerated the treatment well and did not suffer from any health issues during the therapy.

Therapy results indicated a potential pause or dip in growth for the [^{177}Lu]Lu-labelled antibodies followed by fast regrowth; unfortunately, most likely due to hematological side effects and likely due to the lack of targeting several mice died in the group due to poor health, Interestingly, the [^{177}Lu]Lu-IgG had a much higher number of Ki67 and PSA immunoreactive cells than the [^{111}In]In-IgG group. Radiometals such as In^{3+} and Lu^{3+} are trivalent metals, however they differ substantially in their ionic radii and have different coordination numbers [18, 19]. This might influence the interactions of the targeting molecule with the radioimmunoconjugate which might explain difference in PSA expression between [^{177}Lu]Lu-IgG and [^{111}In]In-IgG treated xenograft. However, the reason for this needs to be investigated further. Also,

this experiment needs to be repeated with a large sample sizes to ensure statistical significance.

In conclusion, in the present study, we investigated the outcome of the off-target mechanisms, such as unspecific uptake and EPR effect, as well as different LET using non-specific radiolabeled antibodies. When comparing with already published data we found that specific targeting might negatively influence normal organ uptake when targeting secreted antigens. Also, different linear energy transfers of a radionuclide might have diverse effects on receptor expression and cell proliferation in tumors. The present study demonstrated that when developing antibody-based radiopharmaceuticals parameters other than high affinity toward the antigen is important and should be considered when developing a theragnostic radiopharmaceutical.

Acknowledgements

This study was performed with generous support from the Swedish Cancer Society, Crafoord Foundation, the Swedish Science Council, Mrs. Berta Kamprad's Foundation, the ALF Foundation of the Medical Faculty of Lund University, and the Prostate Cancer Society. We thank Lise-Lotte Kuré for excellent histological work and immunohistochemical labeling performance, Dr. Mohamed Altai for radiolabeling. Kjell Sjöström for providing the unspecific antibody.

Disclosure of conflict of interest

None.

Address correspondence to: Joanna Strand, Department of Oncology, Lund University, Lund, Sweden. E-mail: Joanna.strand@med.lu.se

References

[1] Tsao LC, Force J and Hartman ZC. Mechanisms of therapeutic antitumor monoclonal antibodies. Cancer Res 2021; 81: 4641-4651.

[2] Rycenga HB and Long DT. The evolving role of DNA inter-strand crosslinks in chemotherapy. Curr Opin Pharmacol 2018; 41: 20-26.

[3] Shah A, Rauth S, Aithal A, Kaur S, Ganguly K, Orzechowski C, Varshney GC, Jain M and Batra SK. The current landscape of antibody-based therapies in solid malignancies. Theranostics 2021; 11: 1493-1512.

[4] Baselga J. Monoclonal antibodies directed at growth factor receptors. Ann Oncol 2000; 11 Suppl 3: 187-190.

[5] Thomas A, Teicher BA and Hassan R. Antibody-drug conjugates for cancer therapy. Lancet Oncol 2016; 17: e254-e262.

[6] Vivier D, Sharma SK and Zeglis BM. Understanding the in vivo fate of radioimmunoconjugates for nuclear imaging. J Labelled Comp Radiopharm 2018; 61: 672-692.

[7] Wester HJ and Kessler H. Molecular targeting with peptides or peptide-polymer conjugates: just a question of size? J Nucl Med 2005; 46: 1940-1945.

[8] Heskamp S, Boerman OC, Molkenboer-Kuenen JD, Oyen WJ, van der Graaf WT and van Laarhoven HW. Bevacizumab reduces tumor targeting of antiepidermal growth factor and anti-insulin-like growth factor 1 receptor antibodies. Int J Cancer 2013; 133: 307-314.

[9] Heskamp S, van Laarhoven HW, van der Graaf WT, Oyen WJ and Boerman OC. Radionuclide imaging of drug delivery for patient selection in targeted therapy. Expert Opin Drug Deliv 2014; 11: 175-185.

[10] Elgqvist J, Timmermand OV, Larsson E and Strand SE. Radiosensitivity of prostate cancer cell lines for irradiation from beta particle-emitting radionuclide (1)(7)(7)Lu compared to alpha particles and gamma rays. Anticancer Res 2016; 36: 103-109.

[11] Strand J, Sjostrom K, Lamminmaki UJ, Vilhelmsson Timmermand O, Strand SE and Tran TA. Humanization, radiolabeling and biodistribution studies of an IgG(1)-type antibody targeting uncomplexed PSA for theranostic applications. Pharmaceuticals (Basel) 2021; 14: 1251.

[12] Vilhelmsson Timmermand O, Orbom A, Altai M, Zedan W, Holmqvist B, Safi M, Tran TA, Strand SE and Strand J. A conjugation strategy to modulate antigen binding and FcRn interaction leads to improved tumor targeting and radioimmunotherapy efficacy with an antibody targeting prostate-specific antigen. Cancers (Basel) 2021; 13: 3469.

[13] Veach DR, Storey CM, Luckerath K, Braun K, von Bodman C, Lamminmaki U, Kalidindi T, Strand SE, Strand J, Altai M, Damoiseaux R, Zanzonico P, Benabdallah N, Pankov D, Scher HI, Scardino P, Larson SM, Lilja H, McDevitt MR, Thorek DLJ and Ulmert D. PSA-targeted alpha-, beta-, and positron-emitting immunotheranostics in murine prostate cancer models and nonhuman primates. Clin Cancer Res 2021; 27: 2050-2060.

[14] Ghetie V and Ward ES. Transcytosis and catabolism of antibody. Immunol Res 2002; 25: 97-113.

[15] Johansson AG, Lovdal T, Magnusson KE, Berg T and Skogh T. Liver cell uptake and degradation of soluble immunoglobulin G immune complexes in vivo and in vitro in rats. Hepatology 1996; 24: 169-175.
[16] Agha AH, Schechter E, Roy JB and Culkin DJ. Prostate specific antigen is metabolized in the liver. J Urol 1996; 155: 1332-1335.
[17] Halabi S, Kelly WK, Ma H, Zhou H, Solomon NC, Fizazi K, Tangen CM, Rosenthal M, Petrylak DP, Hussain M, Vogelzang NJ, Thompson IM, Chi KN, de Bono J, Armstrong AJ, Eisenberger MA, Fandi A, Li S, Araujo JC, Logothetis CJ, Quinn DI, Morris MJ, Higano CS, Tannock IF and Small EJ. Meta-analysis evaluating the impact of site of metastasis on overall survival in men with castration-resistant prostate cancer. J Clin Oncol 2016; 34: 1652-1659.
[18] Price EW and Orvig C. Matching chelators to radiometals for radiopharmaceuticals. Chem Soc Rev 2014; 43: 260-290.
[19] Altai M, Strand J, Rosik D, Selvaraju RK, Eriksson Karlstrom A, Orlova A and Tolmachev V. Influence of nuclides and chelators on imaging using affibody molecules: comparative evaluation of recombinant affibody molecules site-specifically labeled with (6)(8)Ga and (1)(1)(1) In via maleimido derivatives of DOTA and NODAGA. Bioconjug Chem 2013; 24: 1102-1109.